Finite element modelling of multi-gas flow in expansive clay

Conference Paper · June 2023

DOI: 10.53243/NUMGE2023-71

4 authors:

Abhishek Gupta
Aalto University
8 PUBLICATIONS **11** CITATIONS
SEE PROFILE

Elke Jacops
SCK CEN - Belgian Nuclear Research Centre
26 PUBLICATIONS **243** CITATIONS
SEE PROFILE

Ayman Abed
Chalmers University of Technology
47 PUBLICATIONS **198** CITATIONS
SEE PROFILE

Wojciech Sołowski
Aalto University
66 PUBLICATIONS **604** CITATIONS
SEE PROFILE

Proceedings 10th NUMGE 2023
10th European Conference on Numerical Methods in Geotechnical Engineering
Zdravkovic L, Kontoe S, Taborda DMG, Tsiampousi A (eds)

https://doi.org/10.53243/NUMGE2023-71

Finite element modelling of multi-gas flow in expansive clay

A. Gupta[1], E. Jacops [2], A. Abed[3], W.T. Solowski[1]

[1] *Department of Civil Engineering, Aalto University, Espoo, Finland*
[2] *Belgian Nuclear Research Centre (SCK CEN), Mol, Belgium*
[3]*Department of Architecture and Civil Engineering, Chalmers University, Gothenburg, Sweden*

ABSTRACT: In a nuclear waste repository, the interaction of groundwater with barrier materials such as canisters, steel liners or waste packages can generate multiple gases. The accumulation of such gases can adversely affect the integrity of an Engineered Barrier System (EBS) and host rock. Therefore, efficient repository modelling requires having a mechanistic understanding and predictive capabilities of these multi-gas interactions and transport processes. This study presents a numerical framework to model gas mixture flow for two incondensable and inert-type gases in expansive clays under hydraulic conditions. The framework is an extension of the finite element code Thebes, incorporating new functions for water retention and gaseous flow behaviour. The current work is limited to only gas flows in soil. For model verification, the study utilises two simplified benchmark tests and one experiment. Each test focuses on specific flow mechanisms i.e., advection, gas phase diffusion or dissolved diffusion. The benchmark test employs COMSOL and/or semi-analytical approaches for verification. The experimental replication uses the diffusion experiment of dissolved gas in Boom clay at constant volume (CH_4 and He), performed by SCK CEN. The presented results show a good match against the experimental data while giving critical insight into gas flow mechanisms in expansive clays.
Keywords: nuclear waste repository; Engineered Barrier System; hydrogen gas; gas mixture

1 INTRODUCTION

The present study is a part of the European Joint Program on Radioactive Waste Management (EURAD): WP6 Gas that focuses on the Engineered Barrier System (EBS), where corrosion of metal structures or aerobic and organic activities can produce multiple gases (OECD-NEA, 2000). These gases, such as vapour, hydrogen, methane, etc., interact at varying concentrations under the repository's thermal-hydraulic and mechanical conditions (THM). The accumulating and migrating gases can create fractures in EBS layers (ex., bentonite) at threshold pressure values. Eventually, this can lead to radioactive gas or radionuclide leakage. Hence, it is essential to create efficient models that can accurately predict gas behaviour in complex subsurface environments. However, most available research treats gas as a single component to predict and study the long-term gas flow behaviour in the repositories (Dagher et al., 2019; Fall et al., 2014; Gerard et al., 2008). On the contrary, various multi-gas flow models exist for applications such as landfill or petroleum gases (Cai et al., 2022; Chamindu Deepagoda et al., 2016; Nastev et al., 2001). Though, these models cannot simulate expansive soils like bentonite (a key EBS layer) under THM conditions.

Thebes is a finite element (FE) code for THM modelling of unsaturated expansive soils (Abed and Sołowski, 2017). The code considers a fully coupled behaviour of solids, as well as air and water in 2 phases (gas and liquid). The recent advancements integrate an additional inert non-condensable gas component into the existing framework. The model employs gas laws, advection, and diffusion flow in two phases (gas and liquid) to simulate the mixing and migration of two gases. Presently, the modifications assume only gas flow and ignore the influence of thermal, mechanical, and water couplings on the gases. Additionally, Thebes adapts EURAD (WP6 Gas) specifications for new water retention and gas flow behaviour functions to facilitate the ongoing research on gas transport in the repository. Due to the limitation of data availability, the study verifies the gas mixture framework by performing simplified 1D (1x1 m^2 geometry) test case simulations in Thebes and a general-purpose multi-physics FE software COMSOL. These trial cases focus on individual gas flow mechanisms: advection and gas phase diffusion. Additionally, Thebes reproduces dissolved gas (CH_4 and He) diffusion experiments by SCK CEN in Boom clay at constant volume (Jacops et al., 2017).

2 THEBES GOVERNING EQUATIONS

Thebes utilises mechanical force balance, conservation of component masses and heat conservation to model the coupled thermal-hydraulic and mechanical behaviour for 3-components (air, water, soil) in a three-phase system (gas, liquid and solid). The code incorporates several constitutive relations that enable the interplay between the couplings. Some important

relations are, for example, the modified Barcelona Basic Model (BBM) with temperature effect for unsaturated expansive soils stress-strain behaviour (Laloui and Cekerevac, 2003; Sánchez et al., 2012), Fourier's heat law for conductive heat transport, Darcy's law for advection, Philip and De Vries (1957) for vapours and Fick's law for non-condensable inert gas diffusion.

The novel enhancements make Thebes competent to handle an additional gaseous component by modifying the current framework. However, presently the extension assumes gas flow under isothermal constant volume soil and no water flow conditions. The section details the derivations and other constitutive functions applicable to the present study. This includes mass balances of two inert gas components (Section 2.1), soil-water retention curve, relative permeability, and gas viscosity functions (Section 2.2). Refer to Abed and Sołowski (2017) for full Thebes derivation.

2.1 Deriving mass conservation of gas components

The governing equations given below are valid for both gas components. For component specific considerations and mass balance expressions, follow Sections 2.1.1 and 2.1.2.

Thebes (Abed and Sołowski, 2017) consider the general form of gas component mass balance (Equation (1)) as a sum of storage, advection, and diffusion terms (ignoring water flow and source term).

$$\frac{\partial(\phi^l \rho^l \omega^l_{g(k)})}{\partial t} + \frac{\partial(\phi^g \rho^g \omega^g_{g(k)})}{\partial t} + \nabla.(\phi^g \rho^g \omega^g_{g(k)} v^g) + \nabla.J^l_{g(k)} + \nabla.J^g_{g(k)} = 0 \tag{1}$$

where, subscript (k = *1, 2*) represents gas-1 or gas-2 components, ϕ^i and ρ^i (i = *l, g*) is the volume fraction and density in liquid (l) and gas (g) phase. Similarly, $\omega^i_{g(k)}$ is the mass fraction of gas-1 or gas-2 in liquid (l) and gas phase (g). v^g (i.e., q^g / nS^g) is a velocity vector of the partial gases in gas phase. n is the porosity, q^g is gas phase specific discharge (Darcy velocity) and S^g is gas degree of saturation. $J^g_{g(k)}$, and $J^l_{g(k)}$ are the gas components (1 or 2) diffusion in gas and liquid phase, respectively. Expanding the storage terms gives:

$$\phi^l \rho^l \omega^l_{g(k)} = nH_{g(k)} S^l \rho^l . (\frac{\rho^l_{g(k)}}{\rho^l}) = nH_{g(k)} S^l \rho^l_{g(k)}$$
$$\phi^g \rho^g \omega^g_{g(k)} = nS^g \rho^g_{g(k)} \quad (where,\ S^l + S^g = 1) \tag{2}$$

where, S^l is liquid degree of saturation. $H_{g(k)}$ (k = *1, 2*) is Henry's volumetric solubility coefficient for gas-1 and gas-2 (Vaunat and Jommi (1997), Equation (3)). Similar to Abed and Sołowski (2017), for simplicity, we assume the density of dissolved gases ($\rho^l_{g(k)}$) in water as equal to the density of the pore-dry gas ($\rho^g_{g(k)}$) in gas phase. Hereafter, ρ_{g1} and ρ_{g2} represents the gas-1 and gas-2 components density for all phases, respectively.

$$H_{g(k)} = H_{c\_(k)} \rho^l_w \frac{RT}{M_w} \tag{3}$$

where, $H_{c\_g(k)}$ (k = *1, 2*) is Henry's solubility coefficient. T is the reference temperature. R is the universal gas constant, and M_w is molar mass of water.

Abed and Sołowski (2017) gives the differential of the degree of saturation (S^l) in the expansion of storage terms in Equation (2).

2.1.1 Gas-1 component mass balance

According to the ideal gas law, the gas-1 density expression and its differential is as follows:

$$\rho_{g1} = \frac{P_{g1} M_{g1}}{RT} = \frac{\rho^l_w g h_{g1} M_{g1}}{RT} \tag{4}$$

$$\frac{\partial \rho_{g1}}{\partial t} = \frac{\rho^l_w g M_{g1}}{RT} \frac{\partial h_{g1}}{\partial t} \tag{5}$$

where, M_{g1} is the molar mass of the gas-1, and P_{g1} is a partial gas-1 pressure. ρ^l_w is water density. h_{g1} is a gas-1 pressure head, that is represented by its equivalent to water pressure.

Further, diffusion of gas-1 for i^{th} phase (gas or liquid) is according to Fick's Law of diffusion:

$$J^i_{g1} = -D^i_{e\_g1} \nabla C^i_{g1} \tag{6}$$

where, C^i_{g1} is the gas-1 concentration, and $D^i_{e\_g1}$ is the effective diffusion of gas-1.

The derivation of dissolved gas-1 mass concentration (Equation (7)) uses the ideal gas law and Henry's solubility coefficient (H_{c_g1}). The expression assumes gas as a dilute solute in water. Here, n^l_w is moles of water in the liquid phase.

$$C^l_{g1} = M_{g1} P_{g1} H_{c\_g1} n^l_w$$
$$(where,\ P_{g1} = \rho^l_w g h_{g1}\ \ \&\ \ n^l_w = \frac{\rho^l_w}{M_w} nS^l) \tag{7}$$

Similarly, for the diffusion in the gas phase (J^g_{g1}) we derive the mass concentration (C^g_{g1}) based on the ideal gas law as follows:

$$C_{g1}^{g} = \frac{M_{g1} P_{g1} n S^{g}}{RT} \tag{8}$$

Expanding Equation (1) and substituting Equations (2-8) gives gas-1 component mass balance as:

$$\begin{aligned} &\left[n(H_{g1} S^{l} + S^{g}) \frac{\rho_w^{l} g M_{g1}}{RT} \right] \frac{\partial h_{g1}}{\partial t} \\ &+ \left[n \rho_{g1} (H_{g1} - 1) \frac{\partial S^{l}}{\partial \psi} \right] \frac{\partial h_g}{\partial t} + \nabla.(\rho_{g1} q^{g}) \\ &-\nabla.\left(D_{e\_g1}^{l} \frac{M_{g1} \rho_w^{l\,2} g n S^{l} H_{c\_g1}}{M_w} \nabla h_{g1} \right) \\ &-\nabla.\left(D_{e\_g1}^{g} \frac{M_{g1} \rho_w^{l} g n (1 - S^{l})}{RT} \nabla h_{g1} \right) = 0 \end{aligned} \tag{9}$$

where, ψ represents a matric suction head (Abed and Sołowski, 2017)

2.1.2 Gas-2 component mass balance

Thebes, by adapting gas component 1 (h_{g1}) and total gas pressure (h_g) as a primary gas variable, calculates the second gas component pressure head (h_{g2}) implicitly in the framework (i.e., h_g - h_{g1}). Considering this, the gas-2 density is as follows:

$$\begin{aligned} &\rho_{g2}^{g} = \frac{M_{g2} P_{g2}}{RT} = \frac{M_{g2} \rho_w^{l} g (h_g - h_{g1})}{RT} \left(\text{ideal gas law} \right) \\ &(\text{where}, P_{g2} = P_g - P_{g1}, P_g = \rho_w^{l} g h_g, P_{g1} = \rho_w^{l} g h_{g1}) \end{aligned} \tag{10}$$

where, P_g, P_{g1} and P_{g2} are total, gas-1 and gas-2 pressures. ρ_{g2}^{g} and M_{g2} represents the gas-2 density and molar mass respectively.

The differential of gas-2 density is as follow:

$$\frac{\partial \rho_{g2}^{g}}{\partial t} = \frac{M_{g2} \rho_w^{l} g}{RT} \left(\frac{\partial h_g}{\partial t} - \frac{\partial h_{g1}}{\partial t} \right) \tag{11}$$

Next, the dissolve diffusion follows the same trend as gas-1 (Equation (12)).

$$J_{g2}^{l} = -D_{e\_g2}^{l} \frac{M_{g2} \rho_w^{l\,2} g n S^{l} H_{c\_g2}}{M_w} \nabla h_{g2} \tag{12}$$

where, $D_{e\_g2}^{l}$ is effective dissolve diffusion for gas-2.

Finally, due to the diffusion constraint condition in the gas phase $\sum_{i=1}^{k} J_i^{g} = 0$ (k components in gas phases), the gas-2 component diffusion is $\nabla.J_{g2}^{g} = -\nabla.J_{g1}^{g}$.

Similar to gas-1, the expression for gas-2 mass balance is as follows:

$$\begin{aligned} &\left[n[S^{g} + H_{g2} S^{l}] \left(\frac{M_{g2} \rho_w^{l} g}{RT} \right) \right] \frac{\partial h_g}{\partial t} \\ &\left[+ n \rho_{g2} [H_{g2} - 1] \frac{\partial S^{l}}{\partial \psi} \right] \\ &-\left[n[S^{g} + H_{g2} S^{l}] \frac{M_{g2} \rho_w^{l} g}{RT} \right] \frac{\partial h_{g1}}{\partial t} + \nabla.(\rho_{g2} q^{g}) \\ &+\nabla.J_{g2}^{l} - \nabla.(J_{g1}^{g}) = 0 \end{aligned} \tag{13}$$

2.2 Some important constitutive relationships

EURAD (WP6 Gas) refers to van Genuchten (1980) expressions for retention curve and relative permeability (Equation (14) and (15)).

$$P_c = \begin{bmatrix} \frac{1}{\alpha} \left((S_e^{*} S_e)^{\frac{-1}{m}} - 1 \right)^{\frac{1}{n}}, if\ S_e \le 1 - \varepsilon \\ \frac{1}{\alpha} \left((S_e^{*} S_e)^{\frac{-1}{m}} - 1 \right)^{\frac{1}{n}} . \frac{(1 - S_e)}{\varepsilon}, if\ 1 - \varepsilon < S_e < 1 \\ 0, if\ S_e = 1 \\ \left(\text{Where}, S_e^{*} = (1 + (\alpha p_e)^{n})^{-m}, \alpha = 1 / P_r, \right. \\ \left. m = 1 - 1/n,\ S_e = \frac{S^{l} - S_{res}^{l}}{S_{sat}^{l} - S_{res}^{l}}, \varepsilon = 0.01 \right) \end{bmatrix} \tag{14}$$

where, S_{sat}^{l} and S_{res}^{l} is the degree of saturation at full saturation and dry state. P_c and P_e is the matric suction and gas entry pressure, respectively. ε, Pr, n, and m are fitting parameters.

$$\begin{aligned} &K_i = K_{ri} K_{i\_sat} \\ &K_{rw} = \sqrt{Se} . \left[\frac{1 - (1 - (S_e^{*} S_e)^{1/m})^{m}}{1 - (1 - S_e^{*1/m})^{m}} \right]^2, \ (1\ if\ S_e = 1) \\ &K_{rg} = \begin{pmatrix} f_g \sqrt{1 - Se} . \left[\frac{(1 - S_e^{*1/m})^{m} - (1 - (S_e^{*} S_e)^{1/m})^{m}}{(1 - S_e^{*1/m})^{m} - 1} \right]^2 \\ , \ (0\ if\ S_e = 1) \end{pmatrix} \end{aligned} \tag{15}$$

where, K_{i_sat} is the saturated hydraulic conductivity of phase i (liquid or gas), and K_{ri} is saturation dependent relative permeability. K_{rw} and K_{rg} are relative permeability of water and gas phases. f_g is the ratio between gas and water intrinsic permeabilities.

Thebes also adapts Herning and Zipperer (1936) gas mixture viscosity (Equation (16)). Here, x_k, μ_k, M_k are molar fraction, viscosity, and molar mass of gas, respectively.

$$\mu^{g} = \left(\sum_{k=1}^{N} x_k \mu_k \sqrt{M_k} \right) / \left(\sum_{k=1}^{N} x_k \sqrt{M_k} \right) \tag{16}$$

3 VERIFICATION TESTS

To verify the gas mixture formulation for isothermal, no water flow and constant volume soil, Thebes simulations replicate two benchmark tests and one experiment. The verification of the benchmark tests is based on COMSOL and/or semi-analytical solution. Each of these simulations targets particular flow mechanisms, namely: a) Gas mixture coupled advection flow (Section 3.1), b) Gas mixture coupled gas phase diffusion (Section 3.2), and c) Gas mixture coupled dissolved diffusion (Section 3.3) by replicating gas diffusion experiment in Boom Clay at constant volume (Jacops et al., 2017).

3.1 Gas mixture coupled advection flow test

A test setup consists of a 1x1 m^2 porous unsaturated material having an upward flow of hydrogen (gas-1) and air (gas-2) due to the difference between fixed top and bottom pressure boundaries and closed vertical walls (see Figure 1). The total simulation time is 1000 sec. Note that the gas pressures referred to hereafter are above the ambient air pressure. For the simulation, Thebes employs 33x33 quadrilateral 4-noded elements. The first test case assumes only advective gas flow. Refer to Table 1 for the test parameters.

Table 1. Soil parameters for benchmark test.

Parameter	Value
Saturation (S^l)	0.604
Porosity (n)	0.4118
Gas intrinsic permeability (K_{intG}) [m^2]	1.0e-16
Water density (ρ_w^l) [kg/m^3]	966.267
Universal Gas const. (R) [J/mol-K]	8.3144
Temperature (T)[K]	293
Molar mass water (M_w) [kg/mol]	0.018016
Molar mass H_2 (M_{g1}) [kg/mol]	0.002016
Molar mass air (M_{g2}) [kg/mol]	0.0280134
g [m/s^2]	9.806
H_2 gas Diffussion ($D^g_{e\_g1}$) [m^2/s]	3.168e-06
Water conductivity (K_{satw}) [m/s]	1.0e-09
H_2 viscosity (μ_{g1}) [Pa.s]	8.87E-06
Air viscosity (μ_{g2}) [Pa.s]	1.81E-05

The pre-defined physics in COMSOL do not allow simulation with two independent gas components. Hence, the COMSOL simulation considers a single representative gas flow (average of gas-1, and 2) and performs the advective flow test by utilising Darcy law physics in an unsaturated porous medium. Further, the analysis uses a triangular quadratic order mesh (930 elements). Table 2 shows averaged COMSOL properties.

Total gas pressure results (Figure 2) suggest a good match between the simulations. The peak pressure at the end of the Thebes test is 196.5 kPa (point A), and the maximum difference is less than 3% (vs COMSOL). The variation may result from using average values in COMSOL for dynamic parameters in Thebes.

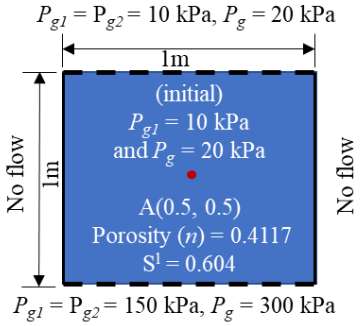

Figure 1. Benchmark test setup.

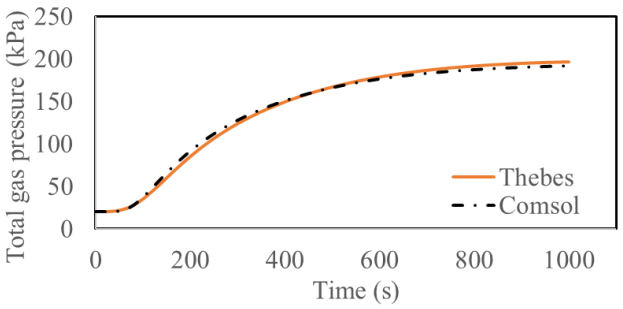

Figure 2. Total gas pressure, advective flow at point A

Table 2. COMSOL parameters for advective flow test.

Parameter	Value
Average gas viscosity* [Pa.s]	1.52E-05
Average specific gas const. [J/kg.K] *Rs = R/Average molar mass*#	553.75

* From Equation (16), *#assuming molar fractions (x_k = 0.5)

3.2 Gas mixture coupled gas phase diffusion test

In this case, the test setup and the Thebes soil parameters remain the same as in Section 3.1 (see Figure 1 and Table 1); only the flow type changes to gas phase diffusion. The total analysis time is 1500 s. COMSOL, however, evaluates only hydrogen component gas diffusion because of coupling limitations. It uses the same 930 triangular elements configuration and employs the transport of diluted species physics in an unsaturated porous medium.

The study derives an analytical expression (Equation (18)) that links air and hydrogen pressure heads to verify the diffusion of air in the gas phase. Subsequently, it obtains the analytical solution of air pressure heads by applying hydrogen gas results from COMSOL. To derive the expression, Equation (17) shows the relation between the storage terms of air and hydrogen component (since, $\nabla.J^g_{g2} = -\nabla.J^g_{g1}$).

$$nS^g \frac{\rho_w^l g M_{g2}}{RT} \frac{\partial h_{g2}}{\partial t} + nS^g \frac{\rho_w^l g M_{g1}}{RT} \frac{\partial h_{g1}}{\partial t} = 0 \qquad (17)$$

Solving Equation (17) for gas-2 pressure head (air) by integrating it in time and using initial conditions gives:

$$h_{g2} = -\frac{M_{g1}}{M_{g2}} h_{g1} + 1 + \frac{M_{g1}}{M_{g2}} \quad (18)$$

$$(\text{at } t = 0,\ h_{g2} = 1, h_{g1} = 1,\ c = 1 + \frac{M_{g1}}{M_{g2}})$$

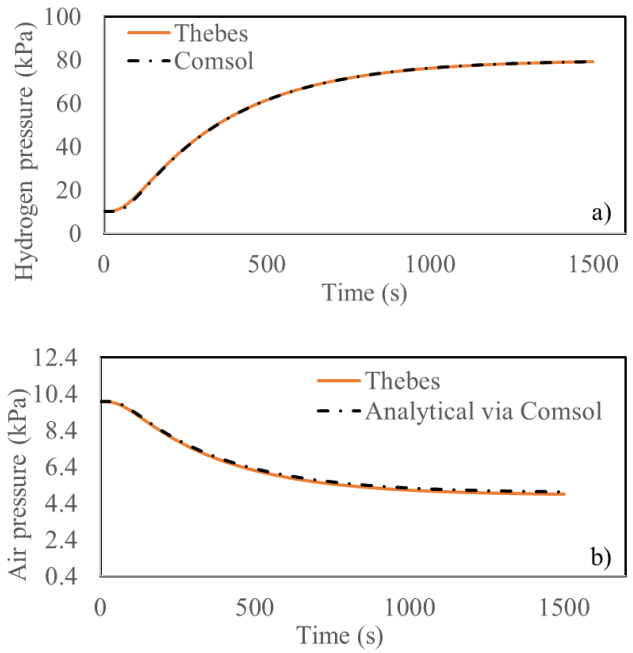

Figure 3. Gas phase diffusion flow at point A: a) Hydrogen pressure, and b) Air pressure

The hydrogen pressure results (Figure 3(a)) show an exact match between Thebes and COMSOL simulation, with a difference of less than 1%. At the end of the simulations, hydrogen pressure at point A reach a peak value of about 74 kPa. Whereas the analytical solution vs Thebes results (Figure 3(b)) for air shows little difference (< 3%). Note that the air pressure boundary and the gradient do not affect the diffusion flow, as the air pressure at point A falls to 4.9 kPa (above 1atm ambient air pressure) at the end of the analysis. Considering Equation (17-18), the dissolved air pressure drops at point A in Thebes simulation represent that the loss in air mass is proportional to the hydrogen mass gain.

3.3 Gas mixture coupled dissolved diffusion

Jacops et al. (2017) examined the influence of gas molecular size and soil pore network in a fully saturated Boom Clay by executing several diffusion experiments with dissolved gases. The present work utilises dissolved methane and helium diffusion experiment. The novel test setup (Figure 4) features a stainless-steel diffusion cell encapsulating a fully saturated Boom Clay sample (sample no. ON-Mol1 84b/K2) of 8 cm diameter, 3 cm height and 0.38 porosity. The porous filter plates connect the sample to two water-gas vessels (filled with half water and half gas) on either side. Vessel-1 and 2 contain methane and helium, respectively. Both vessels maintain a 10 bar pressure. Due to the concentration gradient, methane moves towards vessel-2, while helium migrates to vessel-1.

To simulate the test, Thebes adapts 1D analysis with a 3 cm sample height and 200 elements. It maintains the loading conditions as aforementioned. Table 3 shows the test-specific factors. Refer to Table 1 for other remaining properties.

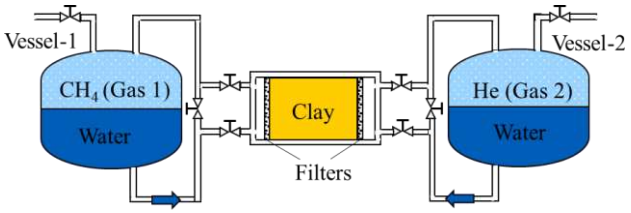

Figure 4. Two gas dissolved diffusion experiment setup

Table 3. Soil parameters for dissolved diffusion

Parameter	Value
Molar mass methane (M_{g1}) [kg/mol]	0.0160
Molar mass helium (M_{g2}) [kg/mol]	0.004
Henry's solubility CH_4 (H_{c_g1}) [Pa^{-1}]	2.45e-10
Henry's solubility He (H_{c_g2}) [Pa^{-1}]	6.84e-11
Temperature (T) [K]	296
CH_4 dissolved diffusion[‡] ($D^l_{e\_g1}$) [m^2/s]	2.5e-10
He dissolved Diffusion[‡] ($D^l_{e\_g2}$) [m^2/s]	1.23e-9
Water density (ρ^l_w) [kg/m^3]	998.0

[‡]From the study by Jacops et al. (2017)

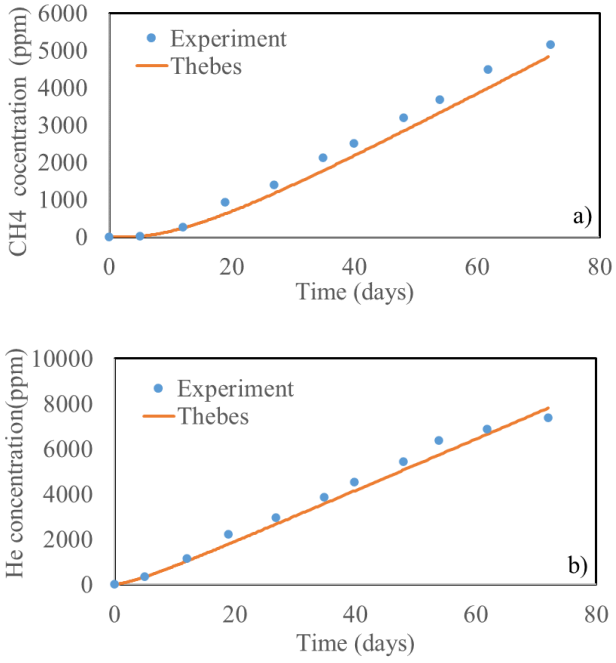

Figure 5. Dissolved gas diffused concentrations: a) Methane in chamber-2, and b) Helium in chamber-1

Figure 5 shows the experimental results of gas concentrations (gas phase) at respective low concentration compartments and compares them with Thebes. Due to the relatively lower diffusion coefficient, methane concentration (5169 ppm, Figure 4(a)) at vessel-2 is relatively lower than Helium in vessel-1 (7391 ppm, Figure 4(b)). In general, Thebes results show a good match against the experiment, the largest difference being 6 % in methane results.

4 CONCLUSIONS

The study introduces a novel two inert and non-condensable gas mixture formulation for isothermal, no water flow and constant volume soil in the framework of FEM code Thebes. Additionally, it incorporates new functions such as retention curve, relative permeability and mixture viscosity. The current research verifies the framework by performing two benchmark tests and one replication of the results of a lab experiment, each targeting different flow types. The former test focuses on advection and gas phase diffusion. For this, the verification employs both COMSOL and/or semi-analytical approaches. The experiment reproduction through Thebes simulations uses a dissolved diffusion experiment of methane and helium in Boom Clay (Jacops et al., 2017). The benchmark test results show negligible differences (less than 3% variation), while the experimental replication performs fairly (6% variation). In general, the analysis confirms the workability of the flow equations. However, the framework testing is still at the preliminary stage, which requires a fully coupled validation to examine the coupling with water and the interplay between the gas mixture flow mechanisms. In future, we further plan to integrate the gas mixture framework with thermal and mechanical conditions. The present research on gas-mixture also indicates potential for Thebes application in landfill or Carbon dioxide sequestration studies.

5 ACKNOWLEDGEMENTS

We thank the EURAD gas project and the Aalto Dean scholarship for funding the research. We further thank SCK CEN for hosting and EURAD for financing the research visit. EURAD has received funding from the European union's Horizon 2020 research and innovation programme under grant agreement n°847593.

6 REFERENCES

Abed, A. A., Sołowski, W. T. 2017. A study on how to couple thermo-hydro-mechanical behaviour of unsaturated soils: Physical equations, numerical implementation and examples. *Computers and Geotechnics*, **92**, 132–155.

Cai, Z., Zhang, K., Guo, C. 2022. Development of a novel simulator for modelling underground hydrogen and gas mixture storage. *International Journal of Hydrogen Energy*, **47**(14), 8929–8942.

Chamindu Deepagoda, T. K. K., Smits, K. M., Oldenburg, C. M. 2016. Effect of subsurface soil moisture variability and atmospheric conditions on methane gas migration in shallow subsurface. *International Journal of Greenhouse Gas Control*, **55**, 105–117.

COMSOL Multiphysics® v. 6.1. www.comsol.com. COMSOL AB, Stockholm, Sweden

Dagher, E. E., Nguyen, T. S., Infante Sedano, J. A. 2019. Development of a mathematical model for gas migration (Two-phase flow) in natural and engineered barriers for radioactive waste disposal. *Geological Society Special Publication*, **482**(1), 115–148.

EURAD: https://www.ejp-eurad.eu/

Fall, M., Nasir, O., Nguyen, T. S. 2014. A coupled hydro-mechanical model for simulation of gas migration in host sedimentary rocks for nuclear waste repositories. *Engineering Geology*, **176**, 24–44.

Gerard, P., Charlier, R., Barnichon, J.-D., Su, K., Shao, J.-F., Duveau, G., Giot, R., Collin, F. 2008. Numerical Modelling Of Coupled Mechanics And Gas Transfer Around Radioactive Waste In Long-Term Storage. In *Journal of Theoretical and Applied Mechanics* 38 (2).

Herning, F., Zipperer, L. 1936. *Calculation of the Viscosity of Technical Gas Mixtures From the Viscosity of the Individual Gases.*

Jacops, E., Aertsens, M., Maes, N., Bruggeman, C., Krooss, B. M., Amann-Hildenbrand, A., Swennen, R., Littke, R. 2017. Interplay of molecular size and pore network geometry on the diffusion of dissolved gases and HTO in Boom Clay. *Applied Geochemistry*, **76**, 182–195.

Laloui, L., Cekerevac, C. 2003. Thermo-plasticity of clays: An isotropic yield mechanism. *Computers and Geotechnics*, **30**(8), 649–660.

Nastev, M., Therrien, R., Lefebvre, R., Gelinas, P. 2001. Gas production and migration in landfills and geological materials. In *Journal of Contaminant Hydrology*, **52**.

OECD-NEA. 2000, June. Gas Generation and Migration in Radioactive Waste Disposal Safety-relevant Issues. *Workshop Proceedings*.

Philip, J., Vries, D. de. 1957. Moisture movement in porous materials under temperature gradients. *Eos, Transactions American Geophysical Union*, **38***(2)*, 222–232.

Sánchez, M., Gens, A., Olivella, S. 2012. THM analysis of a large-scale heating test incorporating material fabric changes. *International Journal for Numerical and Analytical Methods in Geomechanics*, **36**(4), 391–421.

van Genuchten, M. Th. 1980. A Closed-form Equation for Predicting the Hydraulic Conductivity of Unsaturated Soils. *Soil Science Society of America Journal*, **44**(5), 892–898.

Vaunat, J., Jommi C., A. A. G. 1997. Statergy for numerical analysis of the transition between saturated and unsaturated flow conditions. *Numerical Models in Geomechanics*, 297–302.